



# Modeling and optimized design of a parabolic-profile single-mode fiber with ultra-low bending loss and large-mode-area

Haisu Li<sup>a,b</sup>, Guobin Ren<sup>a,b,\*</sup>, Bin Yin<sup>a,b</sup>, Yudong Lian<sup>a,b</sup>, Yunlong Bai<sup>a,b</sup>, Wei Jian<sup>a,b</sup>, Shuisheng Jian<sup>a,b</sup>

<sup>a</sup> Key Lab of All Optical Network & Advanced Telecommunication Network of EMC, Beijing Jiaotong University, Beijing 100044, China

<sup>b</sup> Institute of Lightwave Technology, Beijing Jiaotong University, Beijing 100044, China

## ARTICLE INFO

Available online 29 April 2015

### Keywords:

Single-mode fiber  
Bending loss  
Large-mode-area  
Parabolic-profile

## ABSTRACT

A novel parabolic-profile single-mode fiber with ultra-low bending loss and large-mode-area is proposed in this paper. A modified formula is derived for calculation of bending loss of parabolic-profile single-mode fiber and a performance index is defined as the ratio of bending loss to mode-field-diameter to evaluate fiber performance. The influences of fiber parameters on cutoff wavelength, bending loss and effective mode area are investigated systematically. Simulation results show that the parabolic-profile single-mode fiber could support both an ultra-low bending loss (0.052 dB/turn at bending radii  $R=5$  mm) and a large effective mode area up to  $260 \mu\text{m}^2$  at  $1.55 \mu\text{m}$ , meanwhile maintaining single-mode operation rigorously (cutoff wavelength fixed at  $1.26 \mu\text{m}$ ). This fiber is suitable for compact, portable high power fiber-to-the-home applications.

© 2015 Elsevier B.V. All rights reserved.

## 1. Introduction

With growing interests among researchers in fiber-to-the-home (FTTH) applications driven by rapid development of global high-power optical communication, design and development of novel single-mode (SM) optical fibers with low bending loss and large-mode-area (LMA) are in huge demand [1–5]. Modern-day bend-insensitive fibers (BIFs) that follow the ITU-T Recommendation have been standardized under the G.657 Standard [6], which save the power penalty due to fiber bend at corners of a home. And it is well known that LMA fibers could effectively restrain the fiber nonlinearity for high power applications [7].

Currently, many studies of LMA-BIFs have been presented by tailoring the refractive index (RI) profile or using air holes, such as multi-layer fibers (MLFs) [8–11], trench-assisted step-index fibers (TA-SIFs) [12–20] and hole-assisted fibers (HAFs) [21–23]. However, there are three main drawbacks for these designs. Firstly, fiber fabrication becomes more difficult because of stack-and-draw technique and stringent control of RI profile. Secondly, the scaling of effective mode area ( $A_{\text{eff}}$ ) in such kind of fibers is limited due to cutoff wavelength and detrimental bending effects. As well known, there has been a trade-off between  $A_{\text{eff}}$  and bending loss. Thirdly,

fiber with air holes still has practical issues for adoption.

The fiber design presented in this paper is based on an innovative idea, named parabolic-profile (PP) TA fiber. Such kind of fiber combines the merits of PP fiber and TA fiber. On one hand, a depressed trench around fiber core enhances power confinement in fiber, thereby reducing loss under tight bends. On the other hand, PP fiber is beneficial to enlarging  $A_{\text{eff}}$  [17] and decreasing bending loss meanwhile meeting the rigid condition of cutoff. Up to present, few studies have dealt with the optimization of fiber parameters for maintaining a large  $A_{\text{eff}}$  and bending insensitivity at the same time. With these motivations, we propose a novel PP-SM-LMA-BIF, which avoids air holes or other complex structures. The paper is organized as followings. At the beginning, a modified formula is derived to accurately evaluate the bending loss of PP-TA fiber with bending radii below 10 mm. This theoretical formula could be transplanted into a variety of BIF designs with complex profiles. Next, the mechanism of bending loss control is analyzed, and fiber performances of a SIF and three graded-index fibers (GIFs) (core profiles including PP, Gauss-profile (GP) and cosine-profile (CP)) are compared with fixed cutoff wavelength and core size. Finally, the cutoff wavelength,  $A_{\text{eff}}$  and bending performance affected by parameters of PP-SM-LMA-BIF are systematically discussed. The proposed fiber has a simple and practical structure, which could be a potential candidate for high power FTTH applications.

\* Corresponding author at: Key Lab of All Optical Network & Advanced Telecommunication Network of EMC, Beijing Jiaotong University, Beijing 100044, China.  
E-mail address: [gbren@bjtu.edu.cn](mailto:gbren@bjtu.edu.cn) (G. Ren).

## 2. Fiber structure and theory modeling

The structure of PP-SM-LMA-BIF is shown in Fig. 1, and the distribution of RI profile is

$$n(r) = \begin{cases} n_{\text{clad}}\sqrt{1 + 2\Delta f(r)}, & 0 \leq r < a \\ n_{\text{clad}}, & a \leq r < a + b \\ n_{\text{trench}}, & a + b \leq r < a + b + c \\ n_{\text{clad}}, & r \geq a + b + c \end{cases} \quad (1)$$

where  $a$  is fiber core radius,  $b$  is core-trench distance (i.e. thickness of inner cladding),  $c$  is width of trench,  $n_{\text{core}}$ ,  $n_{\text{trench}}$  and  $n_{\text{clad}}$  express the RIs of core center (i.e.  $r = 0$ ), trench and cladding, respectively.  $\Delta = n_{\text{core}}^2 - n_{\text{clad}}^2 / 2n_{\text{clad}}^2$  means relative RI difference, while  $\Delta n_{\text{core}} = n_{\text{core}} - n_{\text{clad}}$  and  $\Delta n_{\text{trench}} = n_{\text{clad}} - n_{\text{trench}}$  are absolute RI differences of fiber core and trench, respectively. Additionally,  $f(r) = 1 - (r/a)^2$  presents a parabolic function. To evaluate the bending loss of the proposed fiber, an effective approximation is applied for substituting parabolic profile. The fiber core is divided into  $N$  equal length layers as shown in Fig. 1, and the RIs of each layer are sampled values of original PP core. The proposed PP-SM-LMA-BIF could be fabricated by current plasma chemical vapor deposition (PCVD), because PCVD process provides a precise control of index profile. The high index PP core of PP-SM-LMA-BIF could be raised by multi-layer germanium doping, while doping with fluorine creates the depressed index region (trench).

Previous investigations of bending performance of SM fiber focused on single-layer-core multi-layer-cladding structure, and the formula based on perturbation theory has been applied to evaluate the bending loss and validated by experiment results [15,24,25]. In Refs. [15,24] and [25], unperturbed field in the innermost layer and perturbed field in multi-layer-cladding are expressed of Bessel functions  $J_0$  and  $K_0$ , respectively. Unfortunately, the previous theoretical formula is not applicable for PP-SM-LMA-BIF presented in Fig. 1 because of the multi-layer-core structure. In order to meet the continuity of mode field, we modified the regions of unperturbed field and perturbed field. Unperturbed field is core region which is divided into  $N$  layers, and subsequent layers including inner cladding, trench and outer cladding, are considered as the perturbed field. Thus, the redefined perturbed field is readily expressed as  $K_0$  and the continuity condition of mode field is satisfied. Due to fiber bend, the perturbed field can be efficiently coupled back to the unperturbed field. According to the weak guidance approximation, the scalar field of the bending fiber is expanded in Fourier integration of the Airy functions in the direction perpendicular to the curvature plane. The field of the  $q$ th layer is expressed as:

$$\psi_q(x, y) = \frac{1}{2\pi} \int_{-\infty}^{+\infty} [D_q(\zeta)Bi(X_q) + H_q(\zeta)Ai(X_q)] \exp(-i\zeta y) d\zeta \quad (2)$$

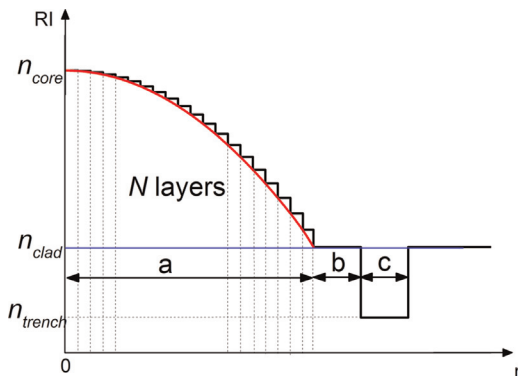


Fig. 1. RI profile of PP-SM-LMA-BIF and its parameters.

where the notations and the expression of  $X_q$  are described in Refs. [24] and [25].  $Ai$  and  $Bi$  are Airy functions of the first kind and the second kind respectively. For the boundary between unperturbed field and perturbed field, we have

$$\begin{aligned} & \int_{-\infty}^{+\infty} \psi_{N+1}(a, y) \exp(i\zeta y) dy \\ &= \int_{-\infty}^{+\infty} K_0(\gamma\sqrt{a^2 + y^2}) \exp(i\zeta y) dy \\ &= \frac{\pi \exp(-a\sqrt{\gamma^2 + \zeta^2})}{\sqrt{\gamma^2 + \zeta^2}} \\ &= D_{N+1}(\zeta)Bi[X_{N+1}(a, \zeta)] + H_{N+1}(\zeta)Ai[X_{N+1}(a, \zeta)] \end{aligned} \quad (3)$$

Combining the continuity condition at boundaries of each adjacent layer of perturbed region and radiation-like condition at infinity [24,25], the attenuation coefficient of bending loss can be finally derived from the interaction of the unperturbed field with the backward evanescent field [15]

$$2\alpha = -\frac{1}{\beta \int_{-\infty}^{+\infty} \psi_0^2 dx} \text{Im}[\psi_{BW}(0, 0)] \quad (4)$$

where  $\beta$  is the unperturbed propagation constant of the fundamental mode of straight fiber,  $\psi_0$  is the unperturbed fundamental mode field, and  $\psi_{BW}(0, 0)$  is the amplitude of the backward evanescent field evaluated on the fiber axis:

$$\psi_{BW}(0, 0) = \frac{1}{2\pi} \int_{-\infty}^{+\infty} H_{N+1}(\zeta)Ai[X_{N+1}(0, \zeta)] d\zeta \quad (5)$$

To validate Eq. (4), we calculate bending loss by finite element method (FEM) for PP-SM-LMA-BIF with bending radii  $R$  lower than 11 mm. The fiber parameters used in both simulations of FEM and theoretical formula are  $a=6 \mu\text{m}$ ,  $b=4 \mu\text{m}$ ,  $c=10 \mu\text{m}$ ,  $\Delta n_{\text{core}} = \Delta n_{\text{trench}} = 0.005$ , and  $n_{\text{clad}} = 1.444$  and  $1.4468$  at wavelengths of  $1.55 \mu\text{m}$  and  $1.31 \mu\text{m}$ , respectively. In common with previous models, the fiber cladding is assumed as infinite. And in FEM simulation, a perfectly matched layer is implemented surrounding the fiber. The elastooptic correction factor is set as 1.28. As shown in Fig. 2, the results from theoretical method agree well with FEM. It is worth noting that the theoretical model is validated for PP-TA-SM fiber with small bending radius. Notice that when bending radius is below 3 mm, an obvious deviation between FEM and theoretical results is observed. This is because perturbation

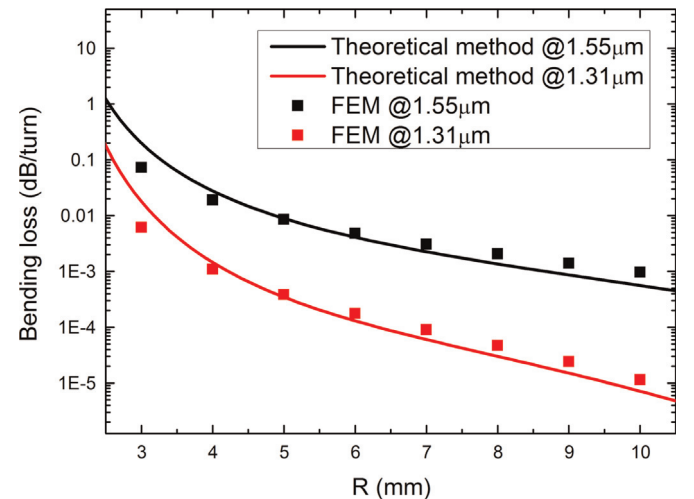


Fig. 2. Comparison of calculated bending losses by theoretical method and FEM as a function of bending radius at wavelengths of  $1.55 \mu\text{m}$  and  $1.31 \mu\text{m}$  for PP-TA-SM fiber.

Download English Version:

<https://daneshyari.com/en/article/1533783>

Download Persian Version:

<https://daneshyari.com/article/1533783>

[Daneshyari.com](https://daneshyari.com)